TUDelft

Delft University of Technology

Accurate small-scale manipulation

Krijnen, Bram; Swinkels, Koen; Brouwer, Dannis M.; Abelmann, Leon; Herder, Just

ACCURATE SMALL-SCALE MANIPULATION

A 3-DoF micro-electromechanical (MEMS) stage has been designed with an innovative integrated feedback system based on thermal sensors. The stage is integrated in the device layer of a silicon-on-insulator-wafer, which means that no assembly is required and the stage can be fabricated using only a single mask. The range of motion is over 160 μm in two directions and 325 mrad of rotation, which exceeds the range of motion of existing MEMS stages by far.

BRAM KRIJNEN, KOEN SWINKELS, DANNIS BROUWER, LEON ABELMANN AND JUST HERDER

1   *One of the fabricated 3-DoF MEMS stages. The device is wire-bonded to a printed circuit board for electrical connection. The die has a size of 8x8 mm² and the positioning stage fits on a wafer surface area of only 6x6 mm².*

From the 1980s on there has been a strong increase in the number of applications that use actuation or sensing based on micro-electromechanical systems (MEMS). One of the first examples is an accelerometer integrated in IC technology. Many applications have been reported since, such as digital micromirror devices for projectors, pressure sensors, gyroscopes, and flow sensors [1] [2]. Due to their small size and low cost, MEMS are also becoming increasingly popular in consumer products, for example in the Nintendo Wii for motion sensing, in digital cameras for image stabilisation, and in smartphones for sports tracking and navigation. MEMS are all around us, nowadays.

MEMS applications do not only benefit from their small volume and low cost, they can also provide superior performance. By scaling down from the macro- to the microscale, the mass of structures ($m \sim r^3$) decreases more rapidly than their stiffness ($k \sim r$), which inherently means a
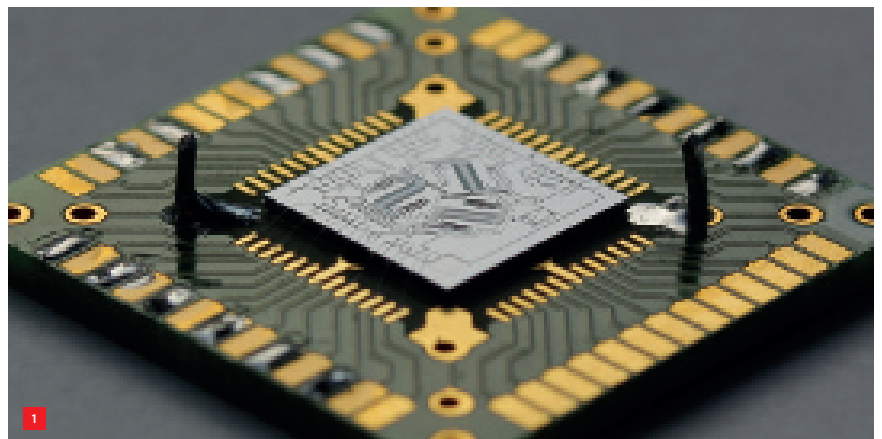
higher eigenfrequency and a faster response time. This opens up a range of interesting applications for MEMS-based positioning stages.

Here, the design, fabrication, and experimental evaluation of a miniature planar positioning stage with integrated feedback (Figure 1) are presented. The complete system has a wafer surface area of only 6x6 mm² and is able to position an end-effector with an in-plane range of motion of 160 μm in x- and y-direction and a rotation of 325 mrad.

Stage motion with three DoFs (degrees of freedom) is realised by means of an eccentric connection of three single-DoF shuttles using leaf springs (Figure 2). The positions of the single-DoF shuttles determine the position and rotation

AUTHORS' NOTE

Bram Krijnen is a mechatronic systems engineer at Demcon in Enschede, the Netherlands. The work presented here is part of his Ph.D. work (2014) at the University of Twente (UT), the Netherlands. Part of this work was laid down at the UT in the M.Sc. thesis (2012) of Koen Swinkels; he is currently starting his own company, focussed on web-based interactive learning. Dannis Brouwer is associate professor in the Mechanical Automation and Mechatronics group at the UT. Leon Abelmann is research group leader in the field of

nanotechnology and magnetism at the Korean Institute of Science and Technology in Saarbrücken, Germany, and professor at the UT and at the Saarland University, Germany. Just Herder is professor at Delft University of Technology, the Netherlands, and at the UT in the field of interactive mechanisms, mechatronics and robotics.

bram.krijnen@demcon.nl
www.demcon.nl
www.utwente.nl
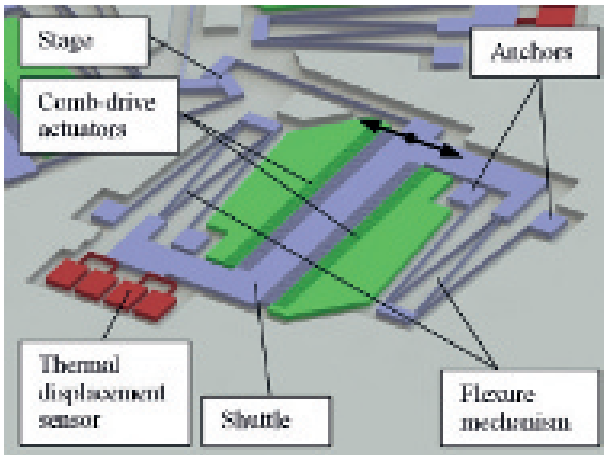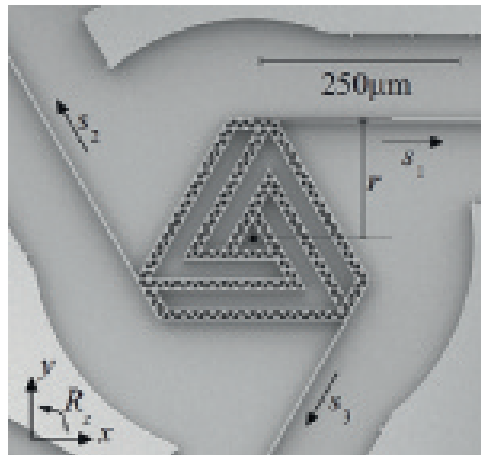
of the 3-DoF stage. The single-DoF shuttles each consist of two electrostatic actuators, two flexure mechanisms and a position sensor for feedback. Actuation is provided by electrostatic comb-drives which are straight-guided by flexure mechanisms. Two flexures are used to prevent rotation of the shuttle [3]. Since a comb-drive actuator can only apply an attractive force, two comb-drives are used per shuttle, to enable motion in opposite directions. The position of each shuttle is measured by a thermal displacement sensor [4] [5].

The sensor consists of two heaters that are resistively heated. Heat is conducted through air towards the 'cold' shuttle. Therefore, the temperature of the heaters changes when the overlap changes and thus the stage position changes. This results in a measurable change in the electrical resistance of the heaters, due to the PTC (positive temperature coefficient) effect in silicon.

Geometry and pull-in
Control of the position of the 3-DoF stage by position control of the three shuttles requires kinematic mapping between the shuttles and the stage. Taking the eccentricity r into account, the positions of the three shuttles (s_1, s_2, and s_3) exactly define the position of the stage in x, y, and R_z (Figure 3). The matrix that defines the kinematic relation between the shuttle and the stage is called the geometric transfer function, GTF. A linearised GTF around the neutral position can be given analytically:

$$\begin{bmatrix} s_1 \\ s_2 \\ s_3 \end{bmatrix} = \text{GTF}_{1A} \cdot \begin{bmatrix} x \\ y \\ R_z \end{bmatrix}$$

$$\text{GTF}_{1A} = \begin{bmatrix} 1 & 0 & -r \\ -\tfrac{1}{2} & \tfrac{1}{2}\sqrt{3} & -r \\ -\tfrac{1}{2} & -\tfrac{1}{2}\sqrt{3} & -r \end{bmatrix}$$

2   *One of the shuttles connected to the 3-DoF stage. Each shuttle is suspended by two double tilted-beam flexures to constrain its movement to a line. The shuttle is actuated by electrostatic comb-drives and the shuttle position is measured by a thermal displacement sensor.*

3   *A scanning electron microscope (SEM) image of one of the fabricated stages. Three equal shuttles are eccentrically connected to the stage with eccentricity r. The positions of the three shuttles s_1, s_2 and s_3 uniquely define the position of the stage in x and y and rotation R_z.*

For large deflections from the neutral position the stage position will no longer behave as a linear function of the shuttle positions. A multi-body model in SPACAR [6] was used to determine the non-linear GTFs of higher order numerically. A wide range of forces was applied to the shuttles; the resulting set of shuttle and stage displacements was used as input for a least-squares curve-fitting algorithm to determine the GTFs and their inverses. For this, the Matlab function *mldivide()* was used. The second-order numerical GTF, for example, has a matrix size of 3x9:

$$\begin{bmatrix} s_1 \\ s_2 \\ s_3 \end{bmatrix} = \text{GTF}_{2N} \cdot \begin{bmatrix} x \\ y \\ R_z \\ x^2 \\ y^2 \\ R_z^2 \\ xy \\ xR_z \\ yR_z \end{bmatrix}$$

Using a GTF of order 4 instead of 1 allows to reduce the error between actual and approximated stage position roughly by a factor of 100, to less than 50 nm and less than 2 mrad for all stage displacements below ±100 μm and all stage rotations below ±450 mrad. Since the complete system is a well-constrained flexure-based design, the device is expected to act repeatably. Determination of the (higher-order) GTFs of the actual devices should enable the reduction of the stage position errors in a similar way.

The major problem that limits the displacement of electrostatically actuated stages is pull-in. Pull-in is the instability that occurs when the lateral electrostatic forces due to the application of an actuation voltage cannot be compensated by the lateral stiffness of the finger or flexure mechanism. This effect can play a role in individual fingers and in entire flexure mechanisms. Both cases are often destructive to the device and need to be avoided.
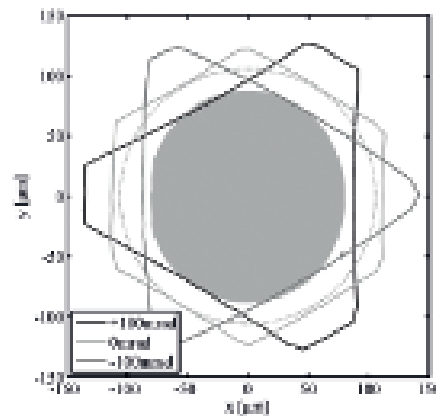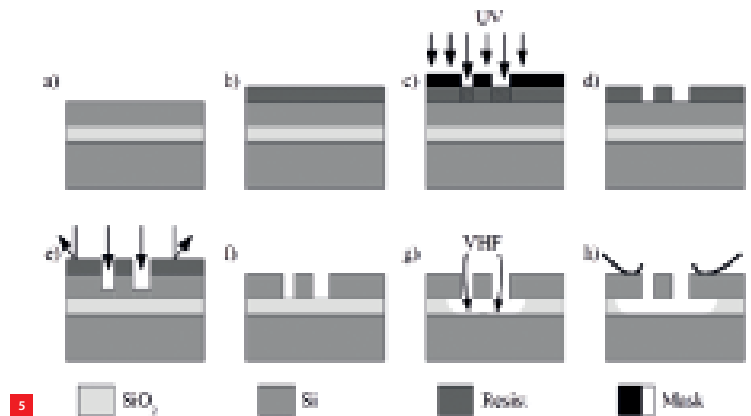
4 *The range of motion of the 3-DoF stage for zero and +/−100 mrad rotation. The dash-dotted circle is the largest circle that fits in the hexagon at zero rotation; the radius of this circle is called the stroke (106 μm). The filled area shows the positions that have been reached experimentally at zero rotation.*

5 *A schematic overview of the fabrication process based on an SOI wafer. The top silicon layer (Si) is structured by DRIE, the insulator layer (SiO$_2$) is etched by VHF. See the text for the complete list of process steps.*

6 *SEM image of the cross-section of a fabricated device, clearly showing the result of the directional DRIE and isotropic VHF etching. The additional protrusion on the vertical edge is probably a splinter as a result of breaking the wafer.*

7 *Identification of the 3-DoF stage in the frequency domain. The first resonance frequencies of the shuttles (~470 Hz) and the R$_z$ mode (1,144 Hz) can be distinguished.*

Finger pull-in can be quite easily avoided by choosing more or thicker comb-drive fingers. Choosing a flexure mechanism is a tougher challenge, since it requires a) a low actuation stiffness, b) a high lateral stiffness in neutral and deflected state, and c) a good approximation of a straight line to avoid asymmetrical electrostatic forces. A double parallelogram flexure (a 'folded flexure') typically gives a good straight-line approximation and low actuation stiffness, but suffers from a large drop in lateral stiffness when deflected. Tilting the beams of the folded flexure slightly inwards constrains the DoF of the intermediate body, which directly results in a higher lateral stiffness at large deflections: the 'tilted folded flexure'.

SPACAR was used to calculate the range of motion of single-DoF shuttles and the complete 3-DoF stage [7]. Electrostatic forces were included in these models. For a 3-DoF stage the range of motion is roughly given by a hexagon (Figure 4); each edge is determined by pull-in of one of the electrostatic actuators. When an additional rotation of the stage is required, the range of motion of the stage becomes more asymmetrical. The largest circle that can be fitted in the hexagon at a specified stage rotation is

called the stroke. At zero rotation the stage has a stroke of 106 μm, for a rotation of 100 mrad this reduces to 84 μm.

Single-mask fabrication

The 3-DoF stages were fabricated in a silicon-on-insulator (SOI) wafer. An SOI wafer consists of three layers: a thick substrate layer, a thin intermediate oxide layer for insulation, and a top single-crystal silicon device layer. The device layer is typically processed to create the desired structures. The process steps are:
a. The starting point is an SOI wafer.
b. Photoresist is applied by spin coating and baking.
c. A mask is prepared by laser writing and the photoresist is exposed to UV light through the mask.
d. The photoresist is developed.
e. Directional deep reactive-ion etching (DRIE) is used for structuring of the silicon device layer.
f. The remaining photoresist is removed.
g. Vapour-phase hydrofluoric acid (VHF) is used for isotropic etching of the buried oxide layer (SiO$_2$).
h. Before use, the devices need to be diced, wire-bonded and packaged.
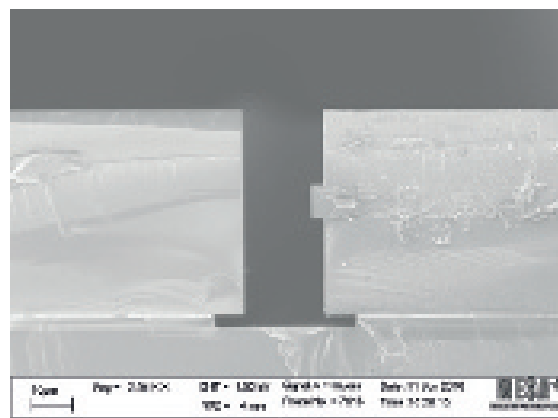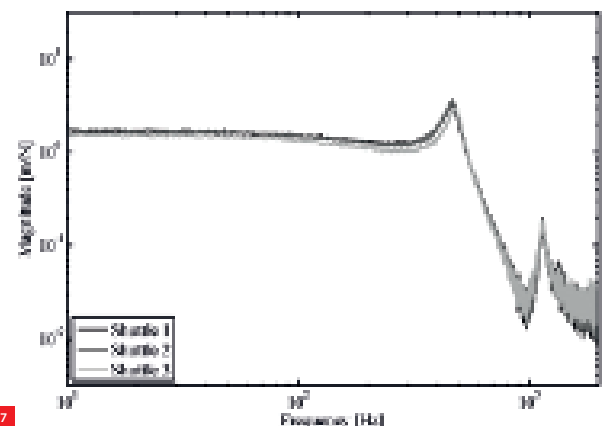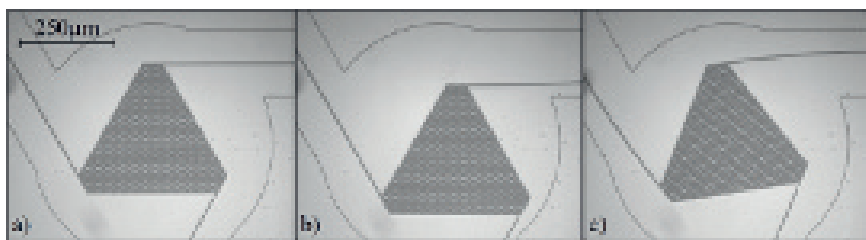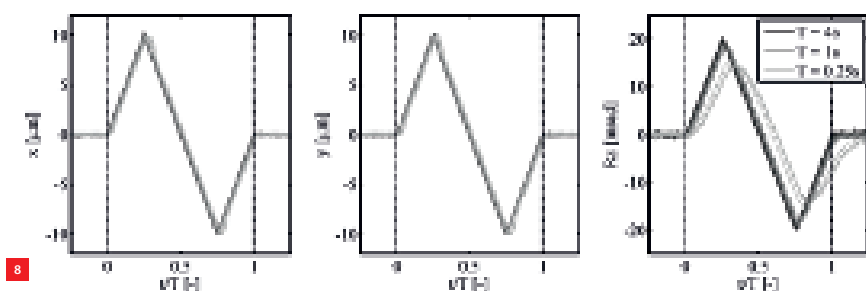
8

9

These steps correspond to the schematic process overview in Figure 5.

In this case the device layer had a thickness of 25 μm, which is therefore also the height of the devices. Lithography followed by DRIE limits the minimum feature size and minimum trench width of the design to 3 μm. An aspect ratio of 3:25 is safe for directional DRIE. VHF etching of the buried oxide layer was used to release thin and perforated structures from the substrate. The cross-section of a fabricated device in Figure 6 shows the result of the directional DRIE and isotropic VHF etching.

Closed-loop positioning

For achieving stable position control of the 3-DoF stage, the system was identified in the frequency domain. White noise was applied to the input of the comb-drive actuators of each shuttle and the sensor response of the corresponding shuttle was measured; the frequency responses from shuttle force to shuttle position are shown in Figure 7.

For giving the frequency response a physical meaning, the actuation voltage is converted to the actuation force ([N]) and the sensor voltage is converted to the shuttle displacement ([m]). Using this transformation, the horizontal line at low frequencies is the inverse of the mechanical stiffness of the shuttles. The stiffness of the shuttles was 0.6 N/m and the first resonance frequencies of 470 Hz correspond to the decoupled modes in x and y. The resonance frequency of 1,144 Hz was found in the identification of each shuttle – it corresponds to the R_z mode of the system, in which the stage shows a pure rotation caused by equal translations of the shuttles.

Controllers with only an integral action were used for position control of the shuttles to eliminate the static error. The cross-over frequency was set to 25 Hz and a first-order motion profile was applied as a setpoint for the controllers. The resulting stage motion was a pure motion in x, y, and R_z of the stage, demonstrating stable control by controlling the positions of the three shuttles. Reduction of the period from 4 s to 0.25 s clearly shows that the rotational movement has a higher stiffness and thus the closed-loop rotational motion shows a larger servo error (Figure 8).

The stroke of the 3-DoF stage was determined by describing circles with increasing radius in the xy-plane. Pure rotations were also applied. The 3-DoF stage was able to reach a stroke of 161 μm in x, 175 μm in y, and a rotation of 325 mrad. An image of the stage in neutral, deflected, and rotated position is given in Figure 9. Since the measurement of the actual pull-in stroke is probably destructive, measurements were stopped at approximately 80% of the expected range of motion.

Asymmetry

Theoretically, the stroke in x and y should be equal, but in practice there is a deviation in the leaf spring thickness as a function of the leaf spring angle on the wafer surface. This results in a different stiffness in x- and y-direction and hence an asymmetric stroke. This deviation was not corrected for during this measurement.

Anyhow, the range of motion of over 160 μm in two directions and 325 mrad of rotation exceeds that of existing MEMS stages by far. ∎

REFERENCES
[1] J.B. Sampsell, "Digital micromirror device and its application to projection displays", *Journal of Vacuum Science & Technology B*, 12(6):3242-3246, 1994.
[2] P. Greiff et al., "Silicon monolithic micromechanical gyroscope", *Solid State Sensors and Actuators*, Vol. 1:966-968, 1991.
[3] S. Awtar et al., "Characteristics of beam-based flexure modules", *Journal of Mechanical Design*, 129(6):625-639, 2007.
[4] B. Krijnen et al., "A single-mask thermal displacement sensor in mems", *Journal of Micromechanics and Microengineering*, 21(7):074007, 2011.
[5] B. Krijnen et al., "Towards accurate small-scale manipulation – A thermal displacement sensor in MEMS", *Mikroniek*, 51(4), pp.5-11, 2011.
[6] J.B. Jonker and J.P. Meijaard, "Spacar – computer program for dynamic analysis of flexible spatial mechanisms and manipulators", in W. Schiehlen (ed.), *Multibody Systems Handbook*, pp. 123-143, Springer, Berlin Heidelberg, 1990.
[7] B. Krijnen et al., "A large-stroke 3dof stage with integrated feedback in mems", *Journal of Microelectromechanical Systems*, 2015 (accepted).